Journal of Photochemistry and Photobiology A: Chemistry 224 (2011) 46–54

Contents lists available at SciVerse ScienceDirect

Journal of Photochemistry and Photobiology A: Chemistry

journal homepage: www.elsevier.com/locate/jphotochem

Hyperbranched polymers as clay surface modifiers for UV-cured nanocomposites with antimicrobial activity

I. Larraza[a], C. Peinado[a], C. Abrusci[b], F. Catalina[a], T. Corrales[a,*]

[a] Polymer Photochemistry Group, Instituto de Ciencia y Tecnología de Polímeros, C.S.I.C. Juan de la Cierva 3, 28006 Madrid, Spain
[b] Departamento de Biología Molecular, Facultad de Ciencias, Universidad Autónoma de Madrid-UAM, Cantoblanco, 28049 Madrid, Spain

ARTICLE INFO

Article history:
Received 28 June 2011
Received in revised form 31 August 2011
Accepted 10 September 2011
Available online 18 September 2011

Keywords:
Hyperbranched polymers
Montmorillonite
UV curing
Nanocomposites
Antimicrobial activity

ABSTRACT

In this work, the influence of organoclays modified with three different hyperbranched polymers (MMT-PEI800Q, MMT-PEI25000Q based on polyethylenimine, and Hybrane MMT-HA1690Q aliphatic polyestheramide), on the photopolymerization reaction of nanocomposites based on HEMA/PEGDMA has been investigated. In general, the clay incorporation increased the reaction rates, associated with the low diffusivity of the monomer into the polymer matrix. The XRD patterns and TEM images of nanocomposites indicated the formation of intercalated/exfoliated structure in the nanocomposites. An enhancement in the thermal stability of nanocomposites was observed by TGA and CL emission, which was related to the great barrier properties of the nanolayers dispersed in the nanocomposites. The antimicrobial activity of the nanocomposites against *Bacillus subtilis* and *Pseudomonas aeruginosa* was tested. For the nanocomposites the inhibition of the adhesion of the two bacteria was observed on comparison to the HEMA/PEGDMA surface, where the colonization by both microorganism was evidenced in SEM images, reflecting no antibacterial activity. The obtained results would indicate that nature of organomodifier in the clay play a more important role in *B. subtilis* and *P. aeruginosa* adhesion processes than stiffness, and the high efficiency against microorganism may be related to the presence of hyperbranched polymers with a high density of quaternary ammonium groups attached to the clay.

1. Introduction

Systems comprising mixtures of polymers and other materials, such organic as inorganic additives, nanoparticles, nanofibers, and mineral sheets, are increasingly touted for their superior properties. Yet, generally, the polymeric components have not been designed explicitly to control interactions with the other ingredients. There is also a need for a more "wholistic" design of nanocomposites.

Three main methods are used to incorporate nanofillers to polymers, including *in situ* polymerization of monomer/clay intercalates, solution-intercalation, and melt-compounding. *In situ* polymerization may be the most desirable method for preparing nanocomposites, since reaction is initiated by the diffusion of a suitable initiator, or by an organic initiator which can be intercalated in the interlayer space of montmorillonite by an ion-exchange mechanism. Photopolymerization is a very promising alternative to prepare nanocomposites [1–4], which is expanding due to the unique advantages (ultrafast reactions, solvent free systems, temporal and spatial control), and because takes place at ambient temperature avoiding any thermal degradation of the alkylammonium salt which is a serious problem in the melt or by *in situ* thermal polymerization. Otherwise, nowadays few studies have been undertaken to investigate the factors controllling the interface polymer/nanoclay which contribute to the design of systems for valued-added applications. Previous works have shown that when organoclays are incorporated into the nanocomposite systems, their properties are often dependent on the nature of modifier used, although no significant changes in the polymerization reaction are induced.

A key factor in the nanocomposite preparation is to compatibilize the matrix and the filler, which will affect the nanostructure (intercalated/exfoliated) and consequently the properties of the nanocomposite. Since most polymers are organophilic, organomodified layered silicates are used to obtain better affinity between the filler and matrix. One of the more common modification methods is the introduction of an ammonium or a phosphonium salt, bearing a suitable organic functionality, inside the interlayer space through a cation exchange reaction. The organic salt substitutes the metal ions present inside the clay mineral galleries, enhances the interlayer between the platelets, and for instance, facilites the intercalation of polymer within galleries, and also is responsible of changes in the surface properties of the clay. For this purpose, attention has been focused to design new strategies to enhance interactions occurring at the interface polymer/nanoclay. For example, free radical polymerization has been initiated from

* Corresponding author. Tel.: +34 912587484; fax: +34 915644853.
E-mail address: tcorrales@ictp.csic.es (T. Corrales).

1010-6030/$ – see front matter © 2011 Elsevier B.V. All rights reserved.
doi:10.1016/j.jphotochem.2011.09.005

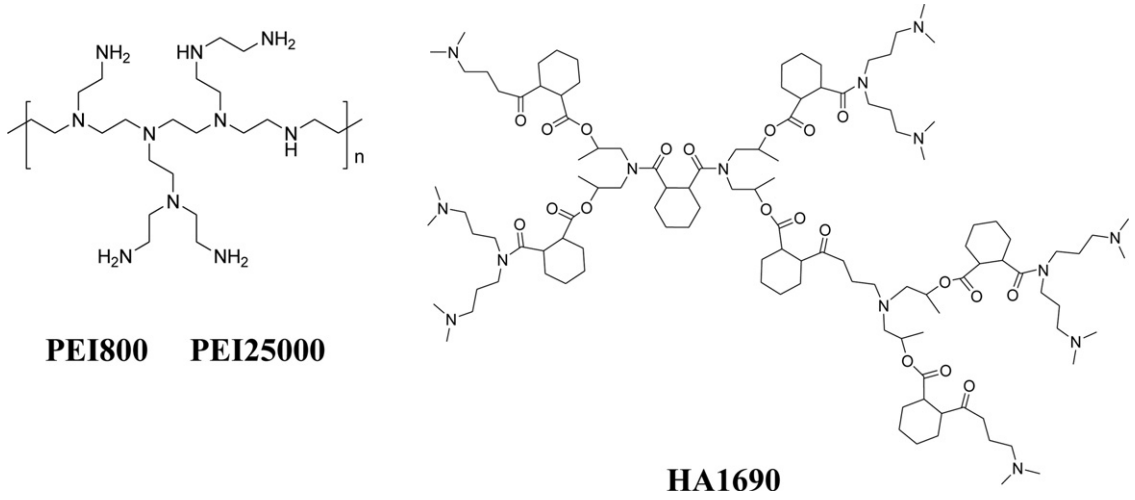

Fig. 1. Structure of hyperbranched PEI800, PEI25000 and HA1690.

quaternized molecules that had been exchanged into the gallery region of a layered silicate and favoured intragallery initiation instead of intergallery [5–7]. Surfmers are used to facilitate the exfoliation during *in situ* polymerization by taking part in the growing step of the polymer chain by copolymerization [8]. An emerging application is the incorporation of positively charged polymers, which can be intercalated in the interlayer space of montmorillonite (MMT) by an ion-exchange mechanism. Polycations have been used for MMT modification, and used as fillers for preparation of polymer/MMT nanocomposites [9]. Although, many works have been reported on the hyperbranched polymer grafted onto the surfaces of silica nanoparticles [10], there are very few examples of the hyperbranched polymer grafted clay in the literature [11].

Hyperbranched polymers (HBPs) are dendritic polymers characterized by a tree-like architecture which confers upon them very different properties compared to their linear counterparts. The structural control in hyperbranched polymers through the adjustment of their degree of branching or by the modification of their end-groups allows the fine-tuning of their physical properties and optimizing them for a great variety of applications, such as multifunctional initiators, nanofillers or medical applications. Recently the use of hyperbranched polymers for applications at surfaces and interfaces has expanded [12]. The potential of HBPs on radiation curing has been put in evidence by a wide number of applications, some of them already commercially developed. Compared to dendrimers, the synthesis of HBPs is easier and more cost-effective. Although some scientists have pointed out that the poorly defined structure and the relatively high polydispersity of HBPs might restrict their applications, novel synthetic methods have recently been developed, in which substantially better-defined HBPs have been obtained with narrow molecular distributions [13].

In this work, the modification of the montmorillonite clay by hyperbranched polymers and its characterization are presented. The study investigates the influence of organoclay on the photopolymerization reaction as well as on the thermal properties of nanocomposites based on acrylate systems. The aim of the work is the development of new approaches for clay-modification in order to improve interactions between polymer and organoclays to further prepare bionanocomposites. The best knowledge over the factors controlling the interface polymer/nanoclay will contribute to the design of systems for high valued-added applications. One of the potential properties of these new materials could be the preparation of antimicrobial surface. Polymers have been used as antimicrobial coatings in many areas, including additives for antifouling paints, biomedical devices and food processing [14,15]. Adhesion of microorganism to a surface is one step of the biofilm formation, which depend on factors such as surface hydrophobicity/hydrophilicity, roughness, charge and functional groups, but the molecular and physical interactions that are involved have not been completely understood. Quaternary ammonium compounds are widely used as cationic disinfectants or biocidal agents to prevent the growth of microorganism [16]. The excess protonated amino groups of hyperbranched polymers that do not interact electrostatically could be effective against colonization of bacteria and may play an important role on safe materials for fighting biofilm. In addition, because biofilm formation requires the initial, stable attachment of a viable bacteria population on a surface, another promising approach to limiting microbial colonization will be provided by regulation of mechanical stiffness of substrata material through incorporation of nanoclay.

2. Experimental

2.1. Materials

The clay employed was montmorillonite k10 (MMT-k10) (surface area of 220–240 m^2/g, Aldrich, C.E.C. = 92 mequiv./100 g), which is a smectite clay with most of its center cations as divalent metal ion. The hyperbranched polymers based on polyethylenimine, PEI800 (ethylenediamine end-capped, M_w 800) and PEI25000, (branched, M_w 25000) were purchased from Aldrich. The aliphatic polyestheramide Hybrane® HA1690 was kindly supplied by DSM. Structure of hyperbranched polymers is shown in Fig. 1. 2-Hydroxyethyl methacrylate (HEMA) and poly(ethylene glycol) dimethacrylate (PEGDMA, M_w 550) from Aldrich were the monomers used. The photoinitiator, bis(2,4,6-trimethylbenzoyl)-phenylphosphineoxide (Irgacure 819) was obtained from BASF. Methyl iodide (MeI) was purchased from Aldrich.

2.2. Quaternary amination of hyperbranched polymers HBPQ

An amount of 3 g hyperbranched polymers (PEI800, PEI25000 and HA1690) were dissolved in 50 ml of dichloromethane and cooled down to 0 °C. Separately, MeI was dissolved in dichloromethane and cooled down also in ice. Then, the solution of MeI, in a 1:10 excess regarding the HBP, was added dropwise to the HBP solution and allowed to reach room temperature. An insoluble yellow compound was obtained by filtering in the reaction carried out, corresponding to quaternized hyperbranched polymers (HPB-Q), namely PEI800Q, PEI25000Q and HA1690Q.

The quaternization of the HBP-Q was analyzed by Nuclear Magnetic Resonance (^{1}H NMR). Spectra were recorded in $CDCl_3$ solution on a Varian INOVA-400 instrument operated at 400 MHz.

Initially, spectra of hyperbranched polymers showed the signal that corresponds to the hydrogen atoms attached to nitrogen, which appeared as a wide singlet centered in 1.81 ppm for PEI800 and PEI25000, and 2.2 ppm for HA1690. After the reaction with MeI, the signal disappeared and a new wide signal corresponding to methyl groups attached to nitrogen was observed between 2.93 and 3.83 ppm for PEI800, 2.86 and 3.62 ppm for PEI25000, and 3.14 and 3.8 ppm for HA1690 respectively.

2.3. Modification of MMT-k10

In order to obtain monocationic montmorillonite, MMT-k10 was suspended in deionized water (50 g/l) and the same amount of NaCl was added to the mixture and stirred for 1 h. The clay was separated by filtration and the procedure was repeated twice. The obtained clay was washed repeatedly with deionized water until no remaining chloride ions were detected by titrating the filtrate with 0.1 N $AgNO_3$ solution. The clay was again suspended in deionized water (10 g/l) and stirred for a week, and then, the clay was let settle for another week. The supernatant fraction was separated from the sediment in the bottom of the container and used for organic modification.

The quaternized hyperbranched polymers were dissolved in acetone and added in 2:1 mass, to a MMT suspension in water (0.5 g/l), and stirred overnight at room temperature. Then, the suspension was filtered under reduced pressure and the obtained HBPQ-modified clays (MMT-PEI800Q, MMT-PEI25000Q and MMT-HA1690Q) were dried under vacuum at 40 °C.

2.4. Synthesis of the nanocomposites

The HBPQ-clays were ground and added to a mixture of monomers, HEMA and PEGDMA (4 wt% respect to HEMA), in different proportions (1, 2 and 3 wt% with respect to HEMA) and placed into an ultrasound bath upon complete dispersion of the clay. Then the photoinitiatior was added (1 wt%) and stirred upon complete solution. The kinetics of photoinitiated polymerization were monitored using a Mettler DSC-821e calorimeter provided with an Hg-Xe LC8 Lightningcure™ Hammamatsu irradiation source. All the irradiation experiments were performed at 25 °C in nitrogen atmosphere.

The nanocomposite samples for TGA and QL analysis were prepared by placing 10 mg of photocurable formulation in 6 mm diameter aluminum pans and irradiated at 365 nm for 30 min. All the samples were post-cured at 80 °C for 24 h.

2.5. Characterization techniques

Diffraction X-ray patterns (XRD) were obtained using an X Bruker D8 Advance diffractometer, with CuKα radiation. The scanning speed and the step size were 0.5°/min and 0.02°, respectively. All the experiments were carried out with 2θ varying from 1° to 30°. The d-spacing between the silicate layers of the clay was calculated using the Bragg's equation.

Transmission electron microscopy (TEM) analyses were carried out on Zeiss 910 microscopy operating at 100 kV.

Scanning electron microscopy (SEM) images were recorded using a Philips XL30 model to observe the stained bacteria on the polymer surface.

Thermal gravimetric analyses (TGA) were performed on both the clays and the resulting nanocomposites using a TGA Q500-0885 (TA Instruments). The heating rate for the dynamic conditions was 5 °C min^{-1}, and the nitrogen flow was maintained constant at 60 ml min^{-1}.

Differential scanning calorimetry (DSC) was performed on a Mettler DSC-821e calorimeter over the temperature range 30–160 °C. The measurements were made at a heating rate of 10 °C min^{-1} in an inert atmosphere of nitrogen and the instrument was calibrated with an indium standard (T_m = 429 K, H_m = 25.75 J g^{-1}). To erase the thermal history of the material, first a heating ramp rate at 20 °C min^{-1} was used, followed by a cooling ramp and a consecutive heating ramp of 10 °C min^{-1} each.

Thermo-oxidative behavior was analyzed from chemiluminescence emission using a CL400 ChemiLume Analyzer from Atlas Electric Device Co. All the materials both clays and composites films were held in a small aluminum pan (20 mm diameter) in the sample cell under a continuous flow of dry oxygen (60 ml min^{-1}). The cell is temperature-controlled and was heated from 25 °C to 250 °C, at a heating rate of 2 °C min^{-1}, for dynamic experiments. In order to assure reproducibility of CL signals the dimensions of the specimens were kept constant: discs of 6 mm diameter and around 1 mm thickness. The films were covered by a lens focusing the emitted light from the sample to the water-cooled photon counting photomultiplier, which was previously calibrated using a radioactive standard provided by Atlas. The light emitted was measured as a function of the temperature [17].

Microindentation measurements were undertaken by using a Vickers indentor attached to a Leitz microhardness tester at 23 °C. A contact load of 0.98 N and a contact time of 25 s were employed. Microhardness (MH), values (in MPa) were calculated according to the relationship [18]: $MH = 2P\sin 68/d^2$, where P (in N) is the contact load and d (in mm) is the arithmetic mean of the two diagonal lengths, $d1$ and $d2$, of the projected indentation area. Diagonals were measured in the reflected light mode within 30 s of load removal, using a digital eyepiece equipped with a Leitz computer-counter-printer (RZA-DO).

2.6. Bacterial attachment

Strains used in this study were *Bacillus subtilis* (DSM-No1088) and *Pseudomonas aeruginosa* (DSM-No288) both strains obtained from the German collection of microorganisms and cell cultures (DSMZ GmbH, Brauschweig, Germany). The bacteria suspensions for inoculums were prepared previously, fixing an absorbance of 1.0 at 550 nm (DO^{550} = 1) in saline buffer (0.9 g/l). One milliliter of this suspension was added to 150 ml of nutrient broth (composition (w/v): 0.5% peptone, 0.3% beef extract and pH adjusted to neutral at 25 °C) in each sterile Erlenmeyer flask (approximately 10^7 cell/ml). In this flask, film strips were placed for a gradient cell adhesion study following a bacterial attachment assay adapted from the established protocol of Tiller et al. [19]. These flasks were incubated at 37 °C under constant shaking at 150 rpm (ELMI, Model sky-line shaker dos-20M) for 2 h. After incubation film samples were rinsed with sterile water and dried. Film strips were placed in Petri dishes containing growth agar (0.7% agar in a yeast/dextrose broth, autoclaved and cooled to 37 °C) and incubated at 37 °C overnight to evaluate the capacity adhesion of the bacteria to the polymer.

3. Results and discussion

3.1. Clay modification

The organomodified nanoclays studied in this work were characterized using XRD and TGA to confirm the intercalation of hyperbranched polymers to the MMTk10 clay. The X-ray diffraction patterns for MMTk10 and organomodified clays are shown in Fig. 2. The unmodified MMTk10 shows a primary silicate (0 0 1)

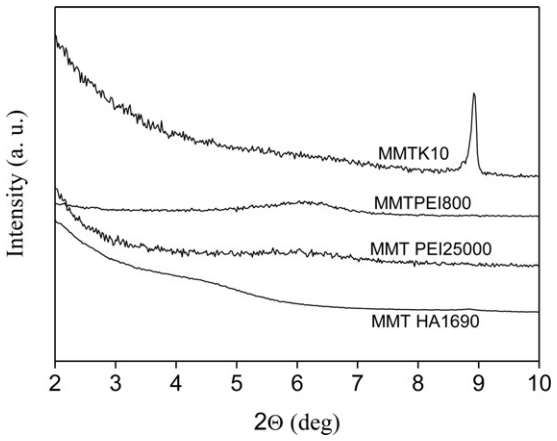

Fig. 2. XRD spectra of MMTk10, MMT-PEI800Q, MMT-PEI25000Q and MMTHA1690Q.

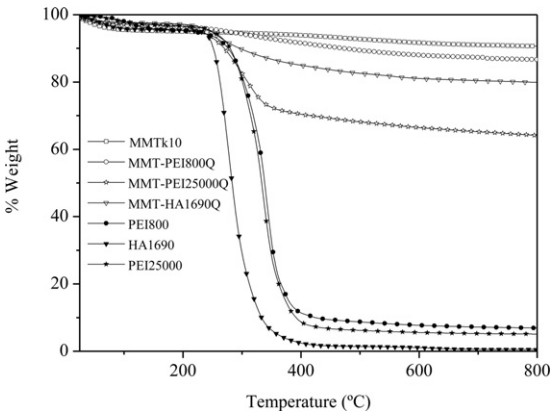

Fig. 3. TGA thermograms of MMTk10, MMT-PEI800Q, MMT-PEI25000Q and MMTHA1690Q, and the hyperbranched polymers PEI800, PEI25000, HA1690.

reflection at 8.9°, which corresponds to a *d*-spacing of 1 nm. Upon the incorporation of the HPBQ, an increase in the interlayer spacing is observed for the organomodified MMT samples when compared to the unmodified clay, which indicates the successful intercalation of the polymeric ammonium salts. The chain length did not affect the basal spacing, as it has been observed previously in the modification of montmorillonite by cationic polyester, where the influence of the side chain was seen to be more significant [9]. MMTk10 modified with the hyperbranched polymers based on polyethylenimine, MMT-PEI800Q, MMT-PEI25000Q, showed an increase in *d*-spacing to 1.45 nm, independently of their molecular weight. The influence of the structure is more significant, and the basal spacing for MMTk10 modified with the aliphatic polyestheramide Hybrane, MMT-HA1690Q, was 1.74 nm. In general, it was observed a significantly broadened reflection for the organomodified clays respect to MMTk10, which reflected an intercalated structure less spatially ordered. That fact would be explained in terms of the structure of organomodifiers, and the presence of several charged groups which could interact electrostatically with different but neighboring platelets surfaces [20].

The thermogravimetric analysis (TGA) of pure clay, and clay intercalated with the HBPQ was undertaken in nitrogen, Fig. 3. As expected, MMTk10 showed a high thermal stability, and a total weight loss of 9% was observed when heating due to the water physically adsorbed in the montmorillonite clay. For the intercalated clays, the weight loss is significantly decreased at temperatures below 200 °C, indicating the lower content of adsorbed water due to the reduced hydrophilicity. When heating up to 800 °C, there is a pronounced weight loss above 200 °C, which indicates the presence of the intercalated organomodifiers on clay platelets, since the decomposition and combustion occurs at the same temperature range and the overall degradation behavior is quite similar to that of pure hyperbranched polymers. The content of the organic components in the modified clays has been determined as the weight loss from 200 °C to 800 °C. At temperatures above 200 °C the influence of water content is eliminated and the process of decomposition and combustion of the intercalated organomodifier takes place. In those conditions, the weight loss for the organomodified clays was 9.7, 17.2 and 32.3% for MMT-PEI800Q, MMT-HA1690Q and MMT-PEI25000Q respectively.

3.2. Photopolymerization behavior of organoclay systems and morphology

The photopolymerization kinetics were monitored by differential scanning calorimetry. The conversion curves as a function of irradiation time for pure HEMA/PEGDMA and containing 1, 2 and 3% of modified clays are showed in Fig. 4. The photopolymerization rate at the peak maximum (R_p^{max}) and the final degree of double bound conversion (α_F) were determined in order to investigate the effects of organomodified clays on the photopolymerization process, Table 1. Kinetic profiles for photopolymerization are conventional, showed an autoacceleration period and then slowed down rate because T_g of system (T_g = 103 °C) is well above polymerization temperature (T = 25 °C) and vitrification of the material takes place.

The addition of organoclay was shown to have no detrimental on the curing reaction. As expected for diffusion-controlled kinetics, a dramatic increase in the polymerization rate is observed at low conversions. This autoacceleration effect is due to the decreased mobility of the growing macroradicals as the viscosity increases,

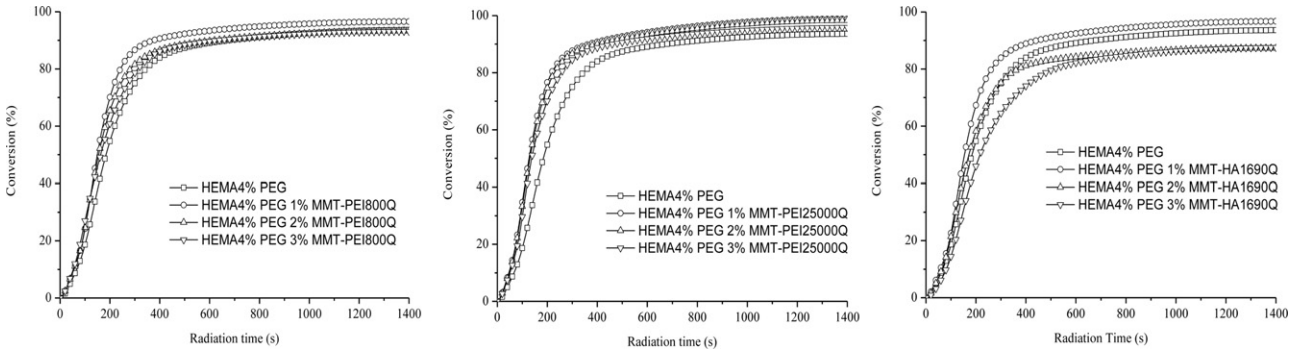

Fig. 4. The double bond conversion versus irradiation time of the neat HEMA/PEGDMA, and with 1, 2, 3 mass% of MMT-PEI800Q, MMT-PEI25000Q and MMTHA1690Q. I = 0.08 mW/cm^2.

Table 1
Analysis result for the photopolymerization of HEMA/PEGDMA in presence of 1, 2, 3% of MMT-PEI800Q, MMT-PEI25000Q and MMT-HA1690Q; and glass transition temperature (T_g) determined by DSC.

HBP surfactant	wt% clay	α_F (%)	R_p^{max} (s^{-1})	T_g (°C)
None	0	94	0.41	104
PEI800Q	1	97	0.54	98
	2	93	0.48	98
	3	93	0.42	103
PEI25000Q	1	99	0.59	97
	2	98	0.58	103
	3	96	0.59	104
HA1690Q	1	98	0.55	99
	2	87	0.43	95
	3	88	0.35	100

which causes a reduction in the termination rate constant, and as a result, the macroradical concentration increases (and, therefore, so does the polymerization rate). The magnitude and onset of the gel effect have been shown to depend on the clay content for the nanocomposites. The clay treatment lead to a widening of the clay interlamellar spacing, and together with the organophilic character of the treated clay, allows an easy penetration of the UV curable monomers into the lamellar structure inducing intercalation and eventually exfoliation. In general, the clay incorporation caused the R_p^{max} increase, associated with the low diffusivity of the monomer into the polymer matrix, and this fact is more noticeable for MMT-PEI25000Q which showed a higher degree of modification and better dispersion in the matrix would be expected. As the clay content increased, the polymerization rate and conversion decreased, which may be due to a reduced penetration of UV radiation into the sample as consequence of presence of large particle aggregates comprised of dozens of platelets.

The addition of a small amount (1%) of the silicate platelets causes a decrease of the glass transition temperature which drops from 104 °C for the pure polymer, to 97–99 °C for the nanocomposite materials. By increasing the clay content to 3%, a T_g value comparable to that of the polymer matrix was obtained, that effect is ascribed to the confinement of the intercalated polymer chains within the clay galleries which restrict polymer chain motions, as result from strong interactions between the clay layers and the polymer chains.

The XRD patterns of nanocomposites containing 2% of modified clays are presented in Fig. 5. The d_{001} peak of the clay in the HEMA/PEGDMA nanocomposites nearly disappeared, indicating the formation of intercalated/exfoliated structure in the nanocomposites. The absence of the (001) peak would suggest that the d_{001} spacing between the layered silicates is intercalated to a

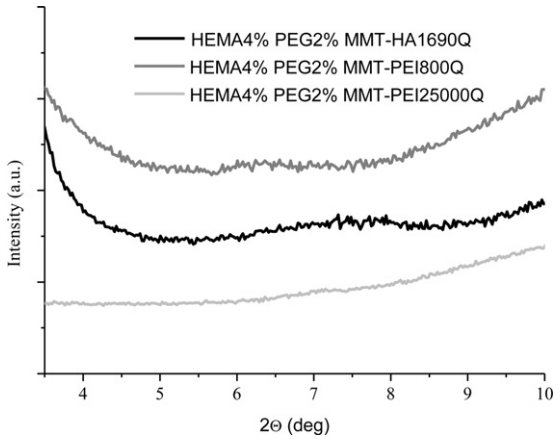

Fig. 5. XRD patterns of the nanocomposites containing 2 mass% of MMT-PEI800Q, MMT-PEI25000Q and MMTHA1690Q.

spacing greater than the measurable range or clay layers are disorderly dispersed in the HEMA/PEGDMA matrix, but also the lack sensitivity at the lower amount of clay loading or random orientation of clay tactoids may be considered. Since XRD analysis gives the macroscopic conformation of a sample, to further investigate the clay dispersion in the polymer matrix, TEM analysis was performed, as shown in Fig. 6. The TEM image reveals that the clay was dispersed uniformly and randomly during the curing process in the polymer matrix, and exfoliated into thin tactoids which contain few clay layers. This result further supports the XRD analysis, the organo-modification makes the layer distance enough for formation of exfoliated morphology.

3.3. Thermal properties of nanocomposites

The thermal degradation behavior of the pure HEMA/PEGDMA and nanocomposites containing modified clays was analyzed by thermogravimetry (TGA) and chemiluminescence emission analysis (CL). The CL has revealed as a very useful technique for the study of polymer degradation, mainly due to its high sensitivity for detecting early stages of oxidation in the polymer when there is neither loss or change in the physical and chemical properties of the material. The chemiluminescence in polymers is due to the light emission that accompanies the thermal decomposition of the thermooxidative degradation products (hydroperoxides), which are formed during processing or service life of the material under ambient conditions. This bimolecular reaction promotes ketone products to its lowest triplet state and the radiative deactivation gives chemiluminescence emission in the visible region. The

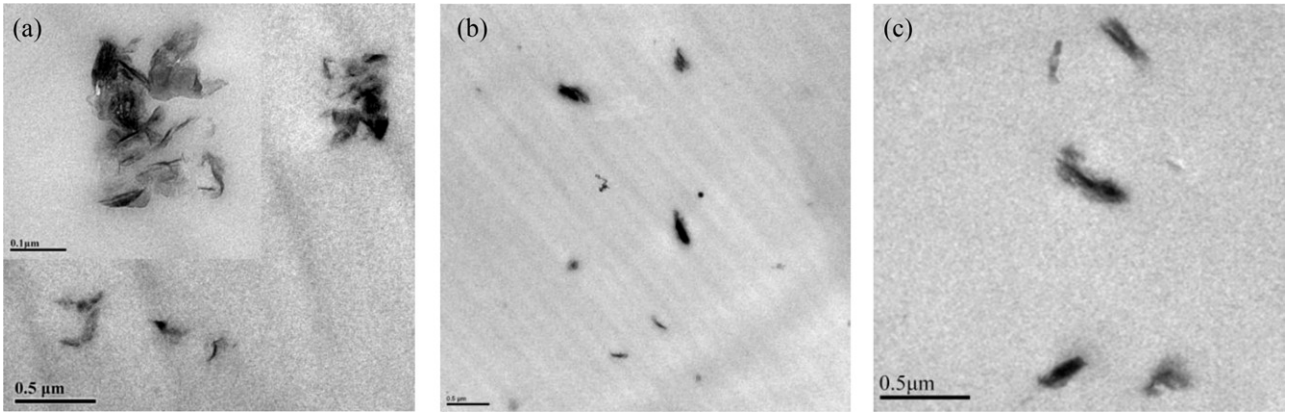

Fig. 6. TEM images of the nanocomposites containing 1 mass% of (a) MMT-PEI800Q, (b) MMT-PEI25000Q and (c) MMTHA1690Q.

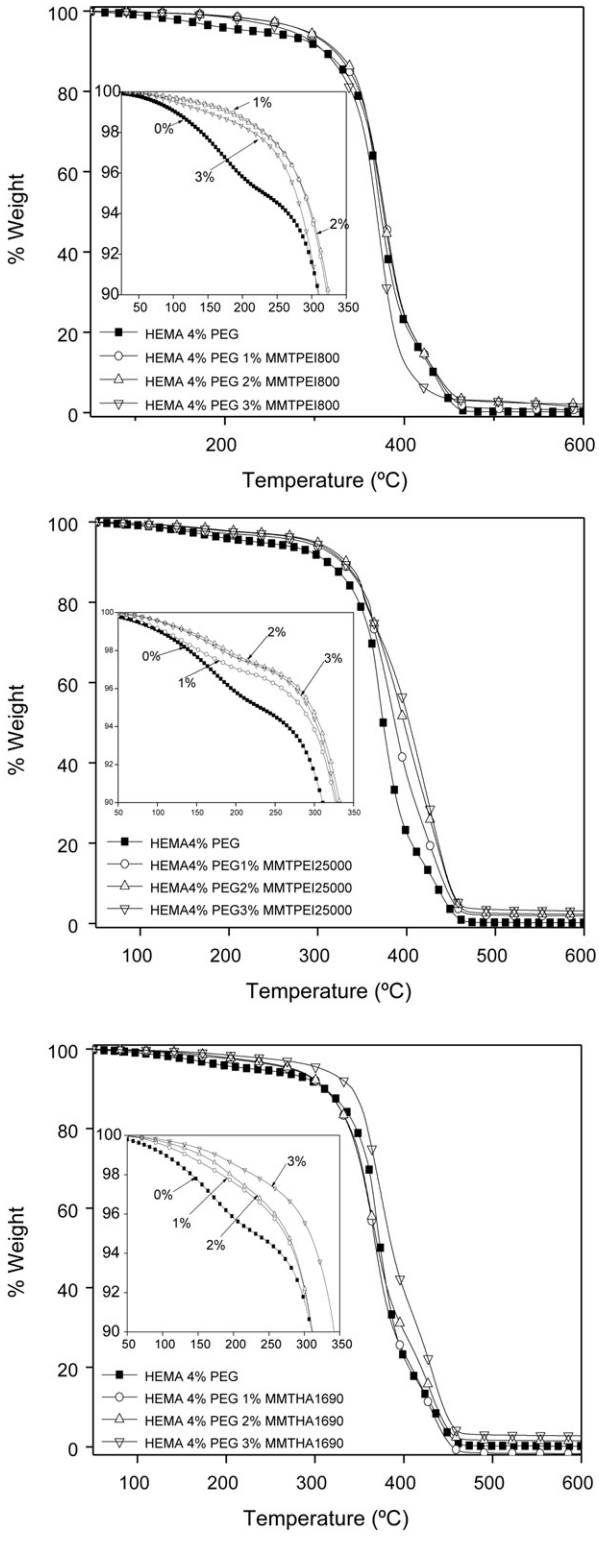

Fig. 7. TGA thermograms of neat HEMA/PEGDMA and nanocomposites containing 1, 2, 3 mass% of MMT-PEI800Q, MMT-PEI25000Q and MMTHA1690Q.

chemiluminescence emission can be related to the hydroperoxide (POOH) content of a polymer [21]. The relationship of several factors such as temperature, molar mass [22,23], oxygen concentration [24], antioxidants [25,26] to changes of the CL intensity in time or with the temperature has been established. During the last decade, significant developments have been achieved in new applications of CL to obtain valuable information related to structure and properties of polymers.

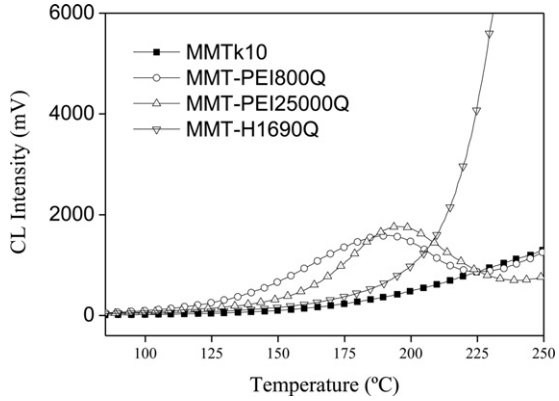

Fig. 8. CL temperature-ramping curves obtained for MMTk10, MMT-PEI800Q, MMT-PEI25000Q and MMTHA1690Q under oxygen.

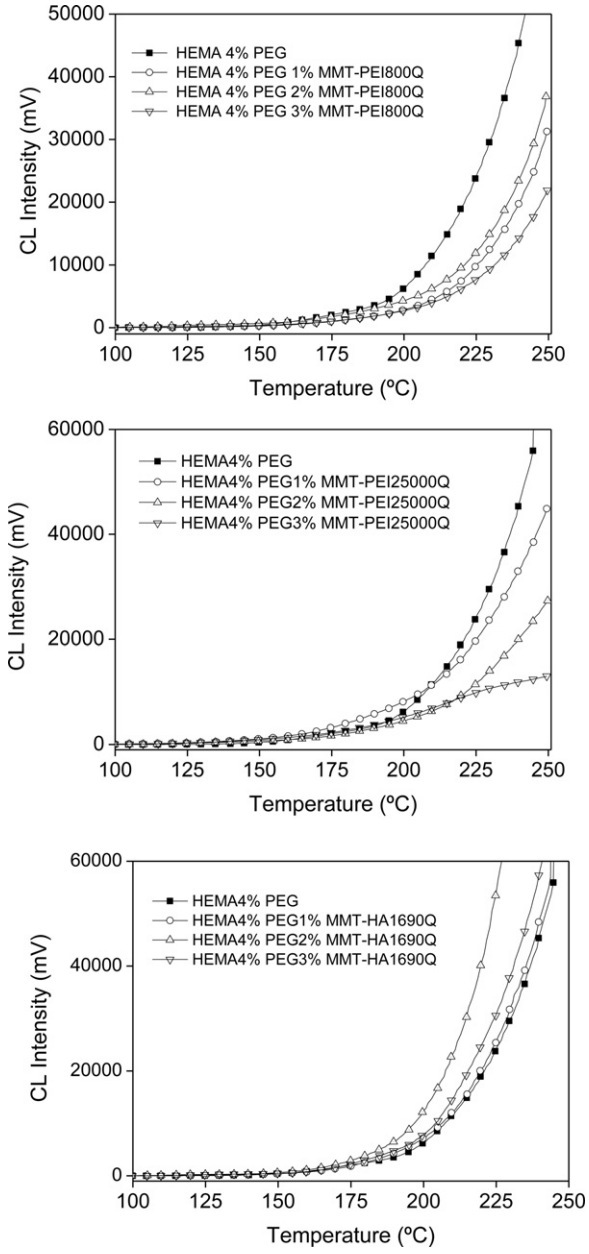

Fig. 9. CL temperature-ramping curves obtained for neat HEMA/PEGDMA and nanocomposites containing 1, 2, 3 mass% of MMT-PEI800Q, MMT-PEI25000Q and MMTHA1690Q.

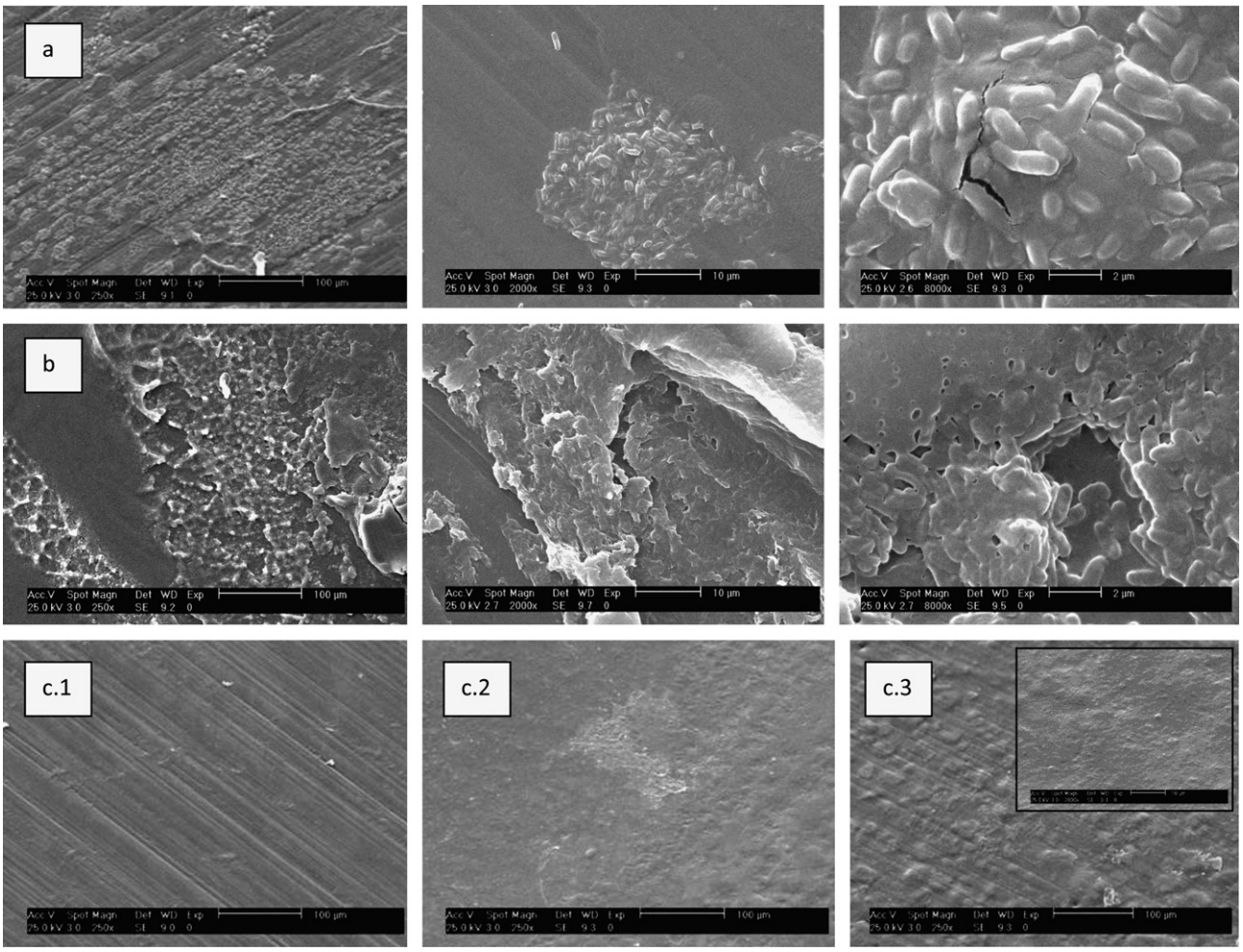

Fig. 10. SEM micrographs of biofilm formation on neat HEMA/PEGDMA samples with (a) *B. subtilis*, (b) *P. aeruginosa*, and biofilm formation with *B. subtilis* on nanocomposites with 1% (c.1) MMT-PEI800Q, (c.2) MMT-PEI25000Q and (c.3) MMTHA1690Q.

By means of thermogravimetric analysis, the mass loss of the nanocomposites was studied as a function of the temperature from 25 to 800 °C under a nitrogen atmosphere. The TGA curves of pure polymer and nanocomposite samples are shown in Fig. 7. The thermal behavior of the nanocomposite is similar to the HEMA/PEGDMA, the TGA curve indicates that there are two stages of decomposition. The first one is due to the loss of adsorbed water, and the addition of clay significantly decreased this weight loss, indicating the lower content of adsorbed water due to the reduced hydrophilicity. With regard to the second stage, at temperature above 300 °C, the nanocomposites have a higher decomposition temperature than pure polymer. This enhancement in the thermal stability is due to the presence of clay nanolayers with high thermal stability and the great barrier properties of the nanolayers dispersed in the nanocomposites to maximize the heat insulation. Those results would be consistent with the XRD results, where the formation of intercalated/exfoliated structure was determined. Comparing the different systems, a better stability is achieved by the samples containing MMT-PEI25000Q, which would be related to the enhanced compatibility with the polymer matrix and better dispersion.

Also, the thermal stability of nanocomposites was studied by means of chemiluminescence analysis. Firstly, temperature-ramping chemiluminescence of the unmodified and organomodified clays was examined under oxygen, in order to determine their possible emission which can affect the polymer chemiluminescence measurement, Fig. 8. All the clays exhibited chemiluminescence emission above 100 °C, and the intensity was markedly enhanced and the onset decreased in presence of the hyperbranched polymers confirming the presence of the modifiers, where hydroperoxide can been generated due to the aliphatic carbons present in their structures. Among the three hyperbranched polymers, aliphatic polyestheramide HA1690 showed a significant chemiluminescence at higher temperatures when compared with the other two polyethylenimines PEI800 and PEI25000. This feature indicated that the emission should be due to the more complex structures of the former. However, these emissions are negligible when the organomodified clays are included in a polymer formulation at the concentrations used in this work. Only in bulk powder the chemiluminescence may be detectable.

By analyzing the chemiluminescence emission of HEMA/PEGDMA sample and nanocomposites it is possible to study the influence of nature of modifier and content of clay in the thermal stability. For the material prepared without montmorillonite, the emission of CL was detected from temperatures above 100 °C that corresponds to the glass transition temperature of the material, where the efficiency of the quantum yield of chemiluminescence emission was enhanced by the increase in mobility of the hydroperoxides which favour the disproportion reaction responsible for the emission. A high intensity of chemiluminescence was observed under oxygen, since in such conditions, the samples are highly oxidised in a diffusion-controlled reaction simultaneously to the emission. Macroradicals react with the oxygen to give peroxy radicals and its concentration will be large

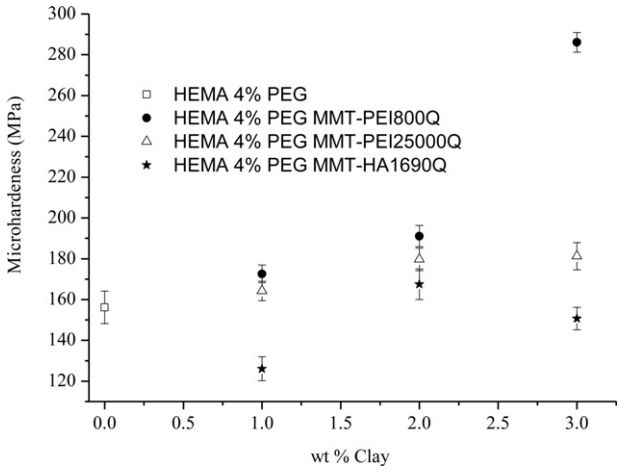

Fig. 11. Microhardness of neat HEMA/PEGDMA and nanocomposites containing 1, 2, 3 mass% of MMT-PEI800Q, MMT-PEI25000Q and MMTHA1690Q.

and the bimolecular termination reaction of two peroxy radicals to give ketone products will be enhanced.

The nanocomposites that contained MMTPEI800 and MMT-PEI25000 presented an improved thermal stability regarding the unloaded material, as it can be seen in Fig. 9. In general, the CL intensity decrease and the onset delay to higher temperature with the content of clay. This means that the presence of reinforcement hinders the diffusion of oxidative species and makes the materials more stable under thermal oxidative conditions. That effect is also more evident for MMTPEI25000 which exhibited lower chemiluminescence emission and would be on good agreement with the higher stability observed by thermogravimetric analysis. Nevertheless, those materials prepared with MMTHA1690 showed similar thermal stability at 1% of clay in all the temperature range, and when increasing clay content a slightly increase in the emission was detected, which may be associated to the presence of large particle aggregates.

3.4. Antimicrobial activity

To analyze the bacteria attachment onto the photogenerated materials, the performance of HEMA/PEGDMA reference as control and nanocomposites with a content of 1% of the organomodified clays were tested. For that purpose, *B. subtilis* and *P. aeruginosa* were used. In Fig. 10 the SEM micrograph of the two bacteria are presented. The nanocomposites with MMTPEI800Q, MMT-PEI25000Q and MMT-HA1690Q markedly inhibited the adhesion of the two bacteria, as compared to the HEMA/PEGDMA surface, where the colonization by both microorganism was evidenced in SEM images, reflecting no antibacterial activity.

It has been reported that surface stiffness, hydrophobic termination and high roughness properties of surfaces can regulate adhesion of bacteria [27]. In order to evaluate potential stiffness contribution to bacterial colonization, microhardness of nanocomposites was analyzed as function of clay content, Fig. 11. Microhardness (MH) measures primarily the resistance of the material to plastic deformation and, accordingly, provides indications regarding local strain. For nanocomposites including MMT-HA1690, similar values to pure polymer were found. A slightly microhardness increase is observed as the clay weight fraction is raised in the nanocomposite materials, with MMT-PEI25000Q even at incorporations as low as 2 wt%. Otherwise, the contribution of the MMT-PEI800Q, is noticeable and MH values increase from 155 to 280 MPa when 3 wt% of clay is added. This behavior can be ascribed to the favourable interfacial characteristics reached during the preparation of materials. The differences of stiffness in the nanocomposites suggested that is not the main property which determines the extent of bacterial attachment. Consequently, the obtained results would indicate that nature of organomodifier in the clay play a more important role in *B. subtilis* and *P. aeruginosa* adhesion processes than stiffness, and the high efficiency against microorganism may be related to the presence of hyperbranched polymers with a high density of quaternary ammonium groups attached to the clay. The activity of the quaternary ammonium compounds has been proposed to involve a general perturbation of lipid bilayer membranes which constitute the bacterial cytoplasmic membrane of Gram negative bacteria [16,28]. Interaction between the positively charged ammonium group with the anionic molecules at the cell surface, would change the permeability of the cell membrane of the microorganism, and the leakage of intercellular components take place.

4. Conclusions

Three different hyperbranched polymers were used in order to modify montmorillonite, and nanocomposites were prepared by photopolymerization of an acrylic matrix with different content of the organomodified clays. In general, the clay incorporation increased the reaction rates, associated with the low diffusivity of the monomer into the polymer matrix, and this fact is more noticeable for MMT-PEI25000Q which showed a higher degree of modification and better dispersion in the matrix analyzed by XRD and TEM. The thermal stability was studied by TGA and CL emission. The nanocomposites showed an enhancement in the thermal stability, related to the great barrier properties of the nanolayers dispersed in the nanocomposites. The novel nanocomposites were tested for antimicrobial activity against *B. subtilis* and *P. aeruginosa*, and inhibition of the adhesion of the two bacteria was observed on comparison to the HEMA/PEGDMA surface, where the colonization by both microorganism was evidenced in SEM images, reflecting no antibacterial activity. The results obtained suggest these materials for potential application in biomedical area.

Acknowledgements

The authors would like to thanks to the MICINN (Spain) for financial support (MAT2009-09671). T.C. would like to thanks to Intramural Project (2006601233). C.A. also thanks to Ramon y Cajal Program.

Appendix A. Supplementary data

Supplementary data associated with this article can be found, in the online version, at doi:10.1016/j.jphotochem.2011.09.005.

References

[1] K. Owusu-Adom, C. Allan Guymon, Macromolecules 42 (2009) 180.
[2] C. Decker, L. Keller, K. Zahouily, S. Benfarhi, Polymer 46 (2005) 6640.
[3] S. Kim, C.A. Guymon, J. Polym. Sci. A: Polym. Chem. 49 (2011) 465.
[4] S. Lv, W. Zhou, S. Li, W. Shi, Eur. Polym. J. 44 (2008) 1613.
[5] L.M. Stadtmueller, K.R. Ratinac, S.P. Ringer, Polymer 45 (2005) 9574.
[6] J. Di, D.Y. Sogah, Macromolecules 39 (2006) 1020.
[7] X. Qin, Y. Wu, K. Wang, H. Tan, J. Nie, Appl. Clay Sci. 45 (2009) 133.
[8] M. Sangermano, N. Lak, G. Malucelli, A. Samakand, R.D. Sanderson, Prog. Org. Coat. 61 (2008) 89.
[9] M. Huskic, E. Zagar, M. Zigon, I. Brnardic, J. Macan, M. Ivankovic, Appl. Clay Sci. 43 (2009) 420.
[10] P. Liu, W.M. Liu, Q.J. Xue, J. Mater. Sci. 39 (2004) 3825.
[11] P. Liu, Appl. Clay Sci. 35 (2007) 11.
[12] C.R. Yates, W. Hayes, Eur. Polym. J. 40 (2004) 1257.
[13] S.E. Stiriba, M.Q. Slagt, H. Kautz, R.J. Kleingebbink, R. Thomman, H. Frey, Chemistry 10 (2004) 1267.
[14] N. Meng, N.-L. Zhou, S.-Q. Zhang, J. Shen, Appl. Clay Sci. 42 (2009) 667.
[15] T. Galya, V. Sedlarik, I. Kuritka, R. Novotny, J. Sedlarikova, P. Saha, J. Appl. Polym. Sci. 110 (2008) 3178.

[16] S.-I. Hong, J.-W. Rhim, J. Nanosci. Nanotechnol. 8 (2008) 5818.
[17] T. Corrales, F. Catalina, C. Peinado, N.S. Allen, E. Fontan, J. Photochem. Photobiol. A: Chem. 5913 (2001) 1–12.
[18] F.J.B. Calleja, Adv. Polym. Sci. 66 (1985) 117.
[19] J.C. Tiller, C.J. Liao, K. Lewis, A.M. Klibanov, Proc. Natl. Acad. Sci. U.S.A. 98 (2001) 5981.
[20] X. Fan, C. Xia, R.C. Advincula, Langmuir 19 (2003) 43481.
[21] N.C. Billingham, E.T.H. Then, P.H. Gijman, Polym. Degrad. Stabil. 42 (1991) 263.
[22] H. Mori, T. Hatanaka, M. Terano, Macromol. Rapid Commun. 18 (1997) 157.
[23] M. Kato, Z. Osawa, Polym. Degrad. Stabil. 65 (1999) 457.
[24] M. Strlic, J. Kolar, B. Pihlar, L. Matisova-Rychla, J. Rychly, Eur. Polym. J. 16 (2000) 2351.
[25] F. Catalina, C. Peinado, N.S. Allen, T. Corrales, J. Polym. Sci. A: Polym. Chem. 40 (2002) 3312.
[26] F. Gugumus, Polym. Degrad. Stabil. 63 (1999) 41.
[27] J.A. Lichter, M. Todd, M. Delgadillo, T. Nishikawa, M. Rubner, K.J. Van Vliet, Biomacromolecules 9 (2008) 1571.
[28] P. Gilbert, L.E. Moore, J. Appl. Microbiol. 99 (2005) 703.